Received: 18 May 2021 | Accepted: 6 October 2021

DOI: 10.1002/jcp.30606

RESEARCH ARTICLE

Journal of Cellular Physiology WILEY

STING-mediated inflammation contributes to Gao binge ethanol feeding model

Ling Wang[1] | Hong-Mei You[1] | Hong-Wu Meng[1] | Xue-Yin Pan[1] | Xin Chen[1] | Yi-Hui Bi[1] | Ya-Fei Zhang[1] | Juan-Juan Li[1] | Na-Na Yin[1] | Zheng-Wei Zhang[2] | Cheng Huang[1] | Jun Li[1]

[1]Inflammation and Immune Mediated Diseases Laboratory of Anhui Province, Anhui Institute of Innovative Drugs, School of Pharmacy, Anhui Medical University, Hefei, China

[2]Department of Neurosurgery, The Second Affiliated Hospital of Anhui Medical University, Hefei, China

Correspondence

Jun Li and Cheng Huang, Inflammation and Immune Mediated Diseases Laboratory of Anhui Province, School of Pharmacy, Anhui Medical University, Hefei 230032, China.
Email: lj@ahmu.edu.cn and huangcheng@ahmu.edu.cn

Abstract

Alcohol metabolism causes hepatocytes to release damage-associated molecular patterns (DAMPs). This includes mitochondrial DNA (mtDNA), which is generated and released from damaged hepatocytes and contributes to liver injury by producing proinflammatory cytokines. STING is a pattern recognition receptor of DAMPs known to control the induction of innate immunity in various pathological processes. However, the expression profile and functions of STING in the Gao binge ethanol model remain poorly understood. We demonstrated that STING is upregulated in the Gao binge ethanol model. STING functions as an mtDNA sensor in the Kupffer cells of the liver and induces STING-signaling pathway-dependent inflammation and further aggravates hepatocyte apoptosis in the Gao binge ethanol model. This study provides novel insights into predicting disease progression and developing targeted therapies for alcoholic liver injury.

KEYWORDS

apoptosis, Gao binge ethanol model, inflammation, mitochondrial DNA, STING

1 | INTRODUCTION

Chronic alcohol consumption and alcoholic liver injury are major causes of mortality and morbidity worldwide and impose a substantial socioeconomic burden (Shim et al., 2020; Stickel et al., 2017). Alcoholic liver injury is a leading cause of chronic liver disease, and has various manifestations, including simple steatosis, hepatitis, and end-stage fibrosis or cirrhosis associated with hepatocellular carcinoma (Bennett et al., 2019; Grabherr et al., 2018). Alcohol intake induces the increase of intestinal permeability which lead to lipopolysaccharide into the portal circulation and trigger inflammatory responses. But in recent years, research has found that sterile inflammation caused by various stimuli induces alcoholic liver injury (Shim et al., 2020). It has been reported that the levels of serum microparticle mitochondrial DNA (mtDNA) are elevated and positively correlated with those of alanine aminotransferase (ALT) and aspartate aminotransferase (AST) in ALD patients (Cai et al., 2017). Chronic-plus-binge ethanol intake activates hepatocytes mtDNA release in patients with alcohol use disorder and in chronically ethanol fed mice (Ma et al., 2020). Damage-associated molecular patterns

Abbreviations: ALT, alanine aminotransferase; AST, aspartate aminotransferase; Clv-caspase3, cleaved-caspase3; CM, cell culture medium; DAMPs, damage-associated molecular patterns; DMXAA, 5,6-dimethylxanthenone-4-acetic acid; IRF3, interferon regulatory factor 3; ip, intraperitoneally; KC, Kupffer cell; mtDNA, mitochondrial DNA; NF-kB, nuclear factor-kB; rAAV, recombinant AAV; STING, stimulator of IFN genes; TBK1, TANK binding kinase 1; TG, hepatic triglyceride.

Ling Wang, Hong-Mei You, and Hong-Wu Meng have contributed equally to this study.

This is an open access article under the terms of the Creative Commons Attribution-NonCommercial-NoDerivs License, which permits use and distribution in any medium, provided the original work is properly cited, the use is non-commercial and no modifications or adaptations are made.
© 2021 The Authors. *Journal of Cellular Physiology* published by Wiley Periodicals LLC

(DAMPs) including mtDNA play a critical role in inducing de novo lipogenesis and inflammation through the activation of cellular pattern recognition receptors such as STING (Abe & Barber, 2014).

STING, encoded by TMEM173, is also known as transmembrane protein 173, N-terminal methionine-prolinetyrosine-serine plasma membrane tetra-spanner (Barber, 2014; Woo et al., 2014). It is an innate immune sensor of cytoplasmic double stranded DNA and is highly expressed in immunoregulation-related tissues and cells (Bai & Liu, 2019). Tang et al. reported that the activation of STING triggers apoptosis in mgnant B cells (Tang et al., 2016). Obesity promotes mtDNA release into the cytosol, where it triggers inflammatory responses by activating the DNA-sensing cGAS-cGAMP-STING pathway (Bai et al., 2017). There was a strong correlation between STING expression and upregulation of other proinflammatory genes associated with the senescence-associated secretory phenotype, which favors NF-κB as the predominant pathway downstream of STING in cancer (Z. Dou et al., 2017). The above research shows that STING can promote tumor apoptosis and stimulate the production of inflammatory mediators. In this study, we found that STING was increased in the Gao binge ethanol model. As STING is a sensor of mtDNA, we reasoned that mtDNA may be required to trigger liver injury of the alcoholic liver injury. We, therefore, set out to uncover the functional role of STING in the Gao binge ethanol model. It was reported that activated STING induces genes, including proinflammatory genes, through the STING-TBK1-IRF3/NF-κB pathway, which could be applied into the treatment of infection and tumorigenesis (Liu et al., 2021). Under stimulation, STING dimer traffic from the Endoplasmic reticulum to the Golgi complex for recruitment of TBK1 protein. TBK1 translocates phosphorylated IRF3 and NF-κB to the nucleus, where immune signals are rapidly amplified by IRF3 and NF-κB pathway (Chen et al., 2016). Furthermore, we hypothesized that STING might influence aseptic inflammation through IRF3/NF-κB pathways.

2 | MATERIALS AND METHODS

2.1 | Animal treatment

Male C57BL/6J mice (aged 6–8 weeks, weighing 18–22 g), procured from the Laboratory Animal Center of Anhui Medical University, were approved by the Institutional Animal Experimental Ethics Committee. The mice were housed in a temperature-controlled room (22°C). The mice were randomly divided into CD-treated and EtOH-treated groups (six mice per group). The Gao binge ethanol model of alcoholic liver injury was established as per the guidelines of the National Institute on Alcohol Abuse and Alcoholism (Bertola et al., 2013). All mice were acclimatized for 3 days before experiments. The establishment of the model required a total of 16 days including the adaptation period during which the mice were administered a liquid diet for 3 days and a control diet (CD) comprising ethanol for 13 d to establish the mouse model. The ethyl alcohol (EtOH)-fed mice were administered a 5% v/v ethanol liquid diet containing certain choline and vitamins and gavaged with a single binge dose of ethanol (5 g/kg, 30% ethanol) on the last day. Meanwhile, the CD-fed mice were administered control liquid diets fortified with certain choline/vitamins and gavaged with isocaloric maltose-dextrin on the last day. All diets were freshly prepared every day. The mice were exsanguinated under anesthesia by inhalation of 5% isoflurane at room temperature, 9 h after the last gavage. The liver tissues and blood from these mice were collected for further analysis, and liver macrophages were isolated. rAAV8-GFP-STING and rAAV8-GFP-empty were procured from Hanbio Biotechnology Co., Ltd. (HY20190921WY-AAV01) and injected via the tail vein as previously described (Nakai et al., 1999). The WT mice were treated with the activator of mouse STING (DMXAA; Selleck), 25 mg/kg/2 days, intraperitoneally [IP]) (Yu et al., 2019). Each in vivo experiment was independently replicated at least three times. The small interfering RNA (siRNA) sequence and short hairpin RNA (shRNA) sequence of Virus vector are as follows:

siRNA sequence: GACTCCTCATCAGTGGTATGGATCA

shRNA sequence:

Top strand: GATCCGACTCCTCATCAGTGGTATGGATCATTCAAGAGATGATCCATACCACTGATGAGGAGTCTTTTTTA

Bottom strand: CGCGTAAAAAAGACTCCTCATCAGTGGTATGGATCATCTCTTGAATGATCCATACCACTGATGAGGAGTCG.

2.2 | Isolation of liver Kupffer cells (KCs) and primary hepatocytes

Liver KCs were extracted according to a previously published protocol (Holt et al., 2008) involving in situ perfusion by Collagenase IV followed by differential centrifugation based on a density gradient. Briefly, a 20-g catheter was inserted through the mouse portal vein, and the inferior vena cava was then cut under anesthesia. The liver was perfused with the perfusion buffer (PB) containing NaCl, KCl, NaOH, and HEPES in H_2O followed by perfusion with a digestion buffer comprising 1× PBC, collagenase IV, pronase E, and $CaCl_2$. After complete digestion, the liver was buffered with PB for 5 min and then stripped and mashed in BSA solution. The liver cells were filtered through a 200-mesh sieve strainer. Macrophages were isolated using 25% Percoll and 50% Percoll. The isolated cells were washed with BSA and transferred to a culture flask containing 5 ml Dulbecco's modified Eagle's medium (DMEM) with 10% fetal bovine serum (FBS). Non-adherent cells and culture medium were discarded after the liver macrophages had adhered to the flask surface for 40 min. Finally, TRIzol© or protein cracking liquid was added to each group of isolated cells to extract RNA and protein for the next experiment. In vivo isolation of primary hepatocytes (HEP) was performed according to a previously published protocol (H. Li et al., 2020; Pan et al., 2019).

2.3 | RNA extraction and real-time polymerase chain reaction (PCR)

Total RNA from liver macrophages and RAW264.7 cells was extracted using TRIzol© (Invitrogen) and reverse-transcribed into complementary DNA using the TAKARA kit (Qiagen). Real time-PCR analyses for

messenger RNA (mRNA) levels of mtDNA, STING, IL-1β, IL-6, and TNF-α were performed by the Thermo script Real time-PCR kit (Fermentas) using GAPDH as an internal control. PCR amplification was performed over 40 cycles including denaturation at 95°C for 10 min followed by anneng at 58°C for 20 s and elongation at 72°C for 1 min using Thermo Step One. The mRNA expression levels were calculated by normzation with the GAPDH levels and the expression levels of the control group. The experiment was carried out in triplicate. The sequences of the respective primers used are listed in Table 1.

2.4 | Extraction and quantification of mtDNA in serum and supernatant

mtDNA was isolated from AML12 cells using the Mitochondrial DNA Isolation Kit (BioVision). The concentration of the isolated mtDNA was measured using Nanodrop (Thermo Fisher Scientific) at 260 nm. DNA was extracted from 200 µl of serum and 50 µl AML12 cell culture using the QIAmp DNA mini kit (Qiagen) and ZR Plasmid MiniPrep Kit (Zymo Cat. No. D4016; Zymo Research), according to the manufacturer's instructions. Then mtDNA levels were measured by RT-qPCR. The purity of mtDNA was determined by agarose gel and the circular mtDNA runs ~15–20 kDa on agarose gel.

2.5 | Western blot analysis

The proteins were isolated from liver macrophages and cultured RAW264.7 cells by lysing them in RIPA buffer containing 1% PMSF (Beyotime). The protein concentration was determined using a BCA protein kit (Beyotime). Based on the protein concentration, equal amounts of protein were separated by SDS/PAGE and transferred onto a PVDF membrane (Millipore Corp.) followed by blocking. The following primary antibodies were used in this study: anti-STING (19851-1-AP; Proteintech), anti-BAX (ab32503; Abcam), anti-BAK (#578; CST), anti-Bcl2 (ab182858; Abcam), anti-p65 (#8242S; CST), anti-p-p65 (#3033S: CST), anti-TBK1 (ab40676; Abcam), anti-p-TBK1 (#5483S; CST), anti-caspase3 (ab184787; Abcam), anti-IRF3 (#11904S; CST), anti-p-IRF3 (#37829S; CST), and anti-β-actin (7D2C10; Proteintech). The protein bands were visuzed using an enhanced chemiluminescence detection system (Bio-Rad) and quantified after normzation to internal control β-actin using the ImageJ software (NIH).

2.6 | Serum activity levels of ALT/AST

Liver-related biochemical tests including those for measuring ALT and AST are commonly used for evaluating the liver function. The serum levels of ALT and AST in C57BL/6J mice with Gao binge ethanol feeding were assayed according to the manufacturers' protocols (Nanjing Jiancheng Bioengineering Institute). The absorbance was measured using a Multiskan MK3 (BioTek) microplate reader at 510 nm. The experiment was performed in three replicates.

2.7 | Histopathology

The middle portion of the left lobe of the liver of each C57BL/6J mouse was excised and perfused in 4% paraformaldehyde for at least 24 h. After fixation, the tissues were embedded in paraffin, and 5 µm thick sections were stained with hematoxylin and eosin (H&E) and oil red O for morphological analysis using standard protocols (H. Li et al., 2020).

2.8 | Cell culture

RAW264.7 cells (No.: TCM13) were purchased from the Chinese Academy of Sciences and cultured in DMEM without sodium pyruvate (HyClone) supplemented with 10% FBS (Bovine). The cells were incubated at 37°C in a 5% CO_2 atmosphere.

2.9 | Overexpression and siRNA knockdown of STING

STING overexpression plasmids or STING siRNA (GenePharma) were transfected into RAW264.7 cells using Lipofectamine 2000 reagent (Invitrogen) as per the manufacturers' recommendations. Cells (3 × 105/ml) were seeded in six-well plates and transfected with the STING plasmid or siRNA and control constructs mixed with Lipo2000 transfection reagent according to the manufacturer's protocol. Finally, the mixture was added to the RAW264.7 cells and incubated for 6 h. The cells were cultured with DMEM supplemented with 10% FBS at 37°C in a 5% CO_2 atmosphere. The STING overexpressing or

TABLE 1 Primers used in RT-qPCR

Gene (mouse)	Forward	Reverse
Tmem173	GGTCACCGCTCCAAATATGTAG	CAGTAGTCCAAGTTCGTGCGA
GAPDH	CATTGCTGACAGGATGCAGAA	TCGCCCCACTTGATTTTGGA
IL-1β	TGTGAAATGCCACCTTTTGA	GGTCAAAGGTTTGGAAGCAG
IL-6	GAGGATACCACTCCCAACAGACC	AAGTGCATCATCGTTG TTCATACA
TNF-α	GAGGATACCACTCCCAACAGACC	TGGGAGTAGACAAGGTACAACCC
mtDNA	ACCAAGGCCACCACACTCCT	ACGCTCAGAAGAATCCTGCAAAGAA

knockdown cells were treated with mtDNA (200 ng/ml) for 24 h and then harvested for Western blot analysis, RT-qPCR or other analyses.

The following siRNA sequences were used:

STING-siRNA: GACTCCTCATCAGTGGTATGGATCA

Scramble-siRNA: TTCTCCGAACGTGTCACGTAA.

2.10 | Enzyme-linked immunosorbent assay (ELISA)

RAW264.7 cells were seeded in six-well culture plates and starved for 12 h (3×10^5/well). The cells in different groups were treated with or without mtDNA for 24 h. The culture medium was then collected, and the levels of inflammatory cytokines TNF-α, IL-6, and IL-1β were detected using an ELISA kit according to the manufacturer's instructions (Elabscience Biotechnology Co. Ltd.). Furthermore, inflammatory cytokines in mouse serum were also detected using ELISA.

2.11 | Flow cytometric analysis

Primary hepatocytes were isolated from mice and analyzed by flow cytometry as previously described (Pan et al., 2019). The apoptosis of primary hepatocytes and AML-12 cells was detected by Annexin V-FITC/PE staining using a FACS Cbur flow cytometer (BD Biosciences). The data were analyzed using the CytExpert software (Beckman Coulter).

2.12 | Terminal deoxynucleotidyl transferase-mediated dUTP nick end labeling (TUNEL) staining

To visuze apoptotic cells, liver tissue sections were fixed in 10% buffered formn at room temperature for 25 min, washed twice with PBS containing 0.2% Triton X-100 at room temperature for 5 min. Subsequently, the sections were covered with 100 µl equilibration buffer and equilibrated for 10 min. Next, rTdT reaction mix was added to the section, and each section was covered with a coverslip. The coverslip was then removed, and sne-sodium citrate was added to terminate the reaction. Furthermore, the slides containing the immobilized sections were immersed in 0.3% H_2O_2 for 3–5 min. After being washed three times with PBS, the slides were immersed in 50 µl of TUNEL detection solution at 15–25°C for 60 min. Finally, the sections were incubated with DAPI (Bi Yuntian Biological Technology) for 10 min. Slides were scanned by Panoramic MIDI (3D HISTECH) and viewed by CaseViewer slice software.

2.13 | Statistical analysis

Data were analyzed by Prism 5.0 GraphPad. All in vitro experiments were performed in triplicates, while all in vivo experiments were repeated at least six times. Values have been presented as means ± SEM. The significance of the results was determined by one-way analysis of variance, unpaired *t* test, and Newman–Keuls posthoc test. The significance level was set as $p < 0.05$.

3 | RESULTS

3.1 | Apoptosis of hepatocytes causes the release of mtDNA in Gao binge ethanol model

WT mice were administered either Lieber-DeCarli ethanol or CD for 16 days to examine whether ethanol induced liver injury. Histopathology of liver tissues was investigated using H&E and oil red O staining. The CD-fed mice showed a normal hepatic lobule structure with a regular arrangement of the hepatic cells. However, the EtOH-fed mice displayed a disordered cell arrangement and inflammatory cell infiltration, and oil red O staining revealed hepatic steatosis in the liver tissues of the EtOH-fed mice (Figure S1A). Furthermore, the levels of ALT, AST, and hepatic triglyceride (TG) were higher in the livers of the EtOH-fed mice compared to that in the CD-fed mice (Figure S1B–D). Alcohol induced inflammation in livers of mice. Moreover, the mRNA expression of IL-1β, IL-6, and TNF-α were determined by real-time PCR and ELISA (Figure S1E,F). These data indicate that the Gao binge ethanol model was successfully established.

Next, we used TUNEL staining to detect hepatocyte apoptosis in vivo. The number of apoptotic cells in the liver tissues was greater in the EtOH-fed mice compared to that in the CD-fed mice (Figure 1a). We further investigated the apoptosis of primary hepatocytes isolated from mice using flow cytometry and found that the percentage of apoptotic cells was increased in the EtOH-fed group (Figure 1b). Furthermore, proapoptotic BAX and BAK are found to be activated, cleaved-caspase3/caspase3 activation in the liver tissues (Figure 1c). Total DNA was isolated from the serum of the mice, and the mtDNA levels were found to be markedly elevated after Gao binge ethanol feeding (Figure 1d). To verify that alcohol induces hepatocyte apoptosis to release mtDNA in vitro. The mouse hepatic cell line (AML12 cells) were treated with ethanol, and the amount of mtDNA released into the medium was determined (Figure 1e). These data indicate that alcohol-stimulated apoptosis of hepatocytes leads to the release of mtDNA in Gao binge ethanol model.

3.2 | Upregulation of STING and inflammatory responses in macrophages depends on mtDNA activation

We have previously shown that in the Gao binge ethanol model, damaged hepatocytes release mtDNA which acts as an agonist for STING (Cheng et al., 2020; Fang et al., 2020). We examined STING expression in the livers of Gao binge ethanol feeding mice, the protein and mRNA levels of STING were found to be increased upon EtOH-fed (Figure 2a,b). To elucidate the molecular mechanisms underlying the

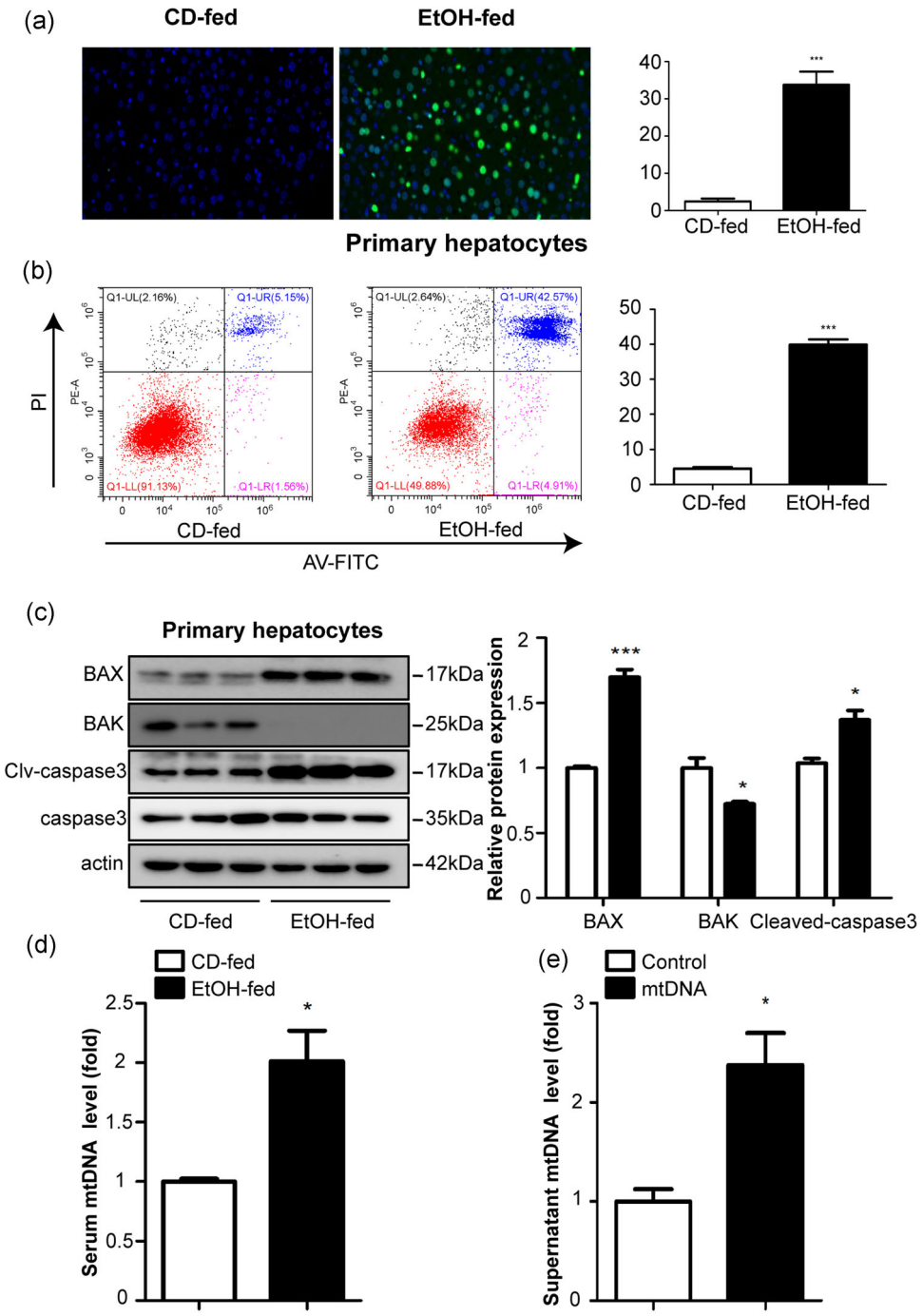

FIGURE 1 Hepatocyte apoptosis results in the release of mitochondrial DNA in Gao binge ethanol model. WT mice were exposed to either liquid (EtOH) or CD for 16 days to induce Gao binge ethanol model. Hepatocyte apoptosis was evaluated using TUNEL assay (a) and flow cytometry (b). Scale bars = 50 μm. Expression of mitochondria-dependent apoptosis signng proteins (Bax, Bak, caspase 3, and cleaved-caspase 3 protein) (c). Total DNA were isolated from serum in the EtOH-fed and CD-fed mice, and mtDNA levels were then measured by RT-qPCR (d). AML12 were incubated for 24 h with or without 200 μM EtOH (Sun et al., 2018). Cells were centrifuged, and mtDNA levels in the supernatant were determined by real time-PCR (e). Data represent the mean ± SEM. *$p < 0.05$, ***$p < 0.001$, as indicated. For all panels, data represent the mean ± SEM for three independent experiments

regulation of hepatic infiltration in Gao binge ethanol model, we analyzed the STING expression in KCs and primary hepatocytes. Western blot and real-time PCR showed that the protein and mRNA levels of STING were increased in the macrophages isolated from the mice with Gao binge ethanol feeding (Figure 2c,d), slightly changed in primary hepatocytes (Figure 2e,f). The mRNA and protein levels of STING were significantly increased in RAW264.7 cells cultured with mtDNA (200 ng/ml) (Figure 2g,h). Furthermore, results from ELISA and real-time PCR assays suggested increased inflammatory cytokines, including TNF-α, IL-6, and IL-1β in the mtDNA-treated RAW264.7 cells and it's

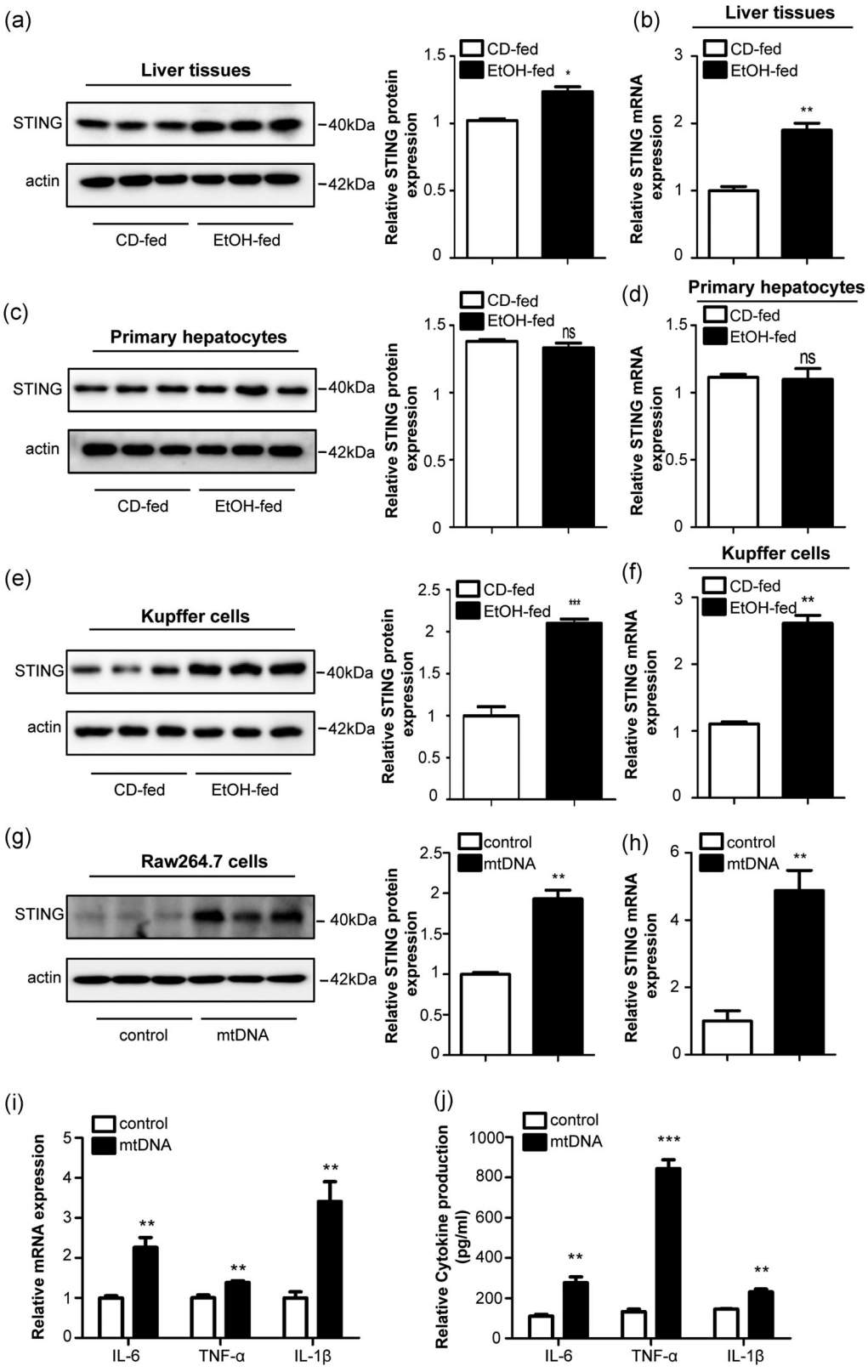

FIGURE 2 Upregulated expression of STING in vivo and in vitro. The protein (a) and mRNA (b) levels of STING in liver tissues from mice. Primary KCs and primary hepatocytes were isolated from C57BL/6J mice. Protein and mRNA expression of STING in KCs (c, d) and hepatocytes (e, f). RAW264.7 cells were incubated for 24 h with or without mtDNA (200 ng/ml). Protein and mRNA expression of STING in RAW264.7 cells (g, h). Graphs show mRNA (i) and protein (j) expression of TNF-α, IL-6, and IL-1β. Representative pictures are shown. Data represent the mean ± SEM. $^{*}p < 0.05$, $^{**}p < 0.01$, $^{***}p < 0.001$, as indicated. For all panels, data represent the mean ± SEM for three independent experiments. KC, Kupffer cell; mRNA, messenger RNA; ns, not significant

supernatants (Figure 2i,j). These results indicate that STING was upregulated in vivo and in vitro.

3.3 | Recombinant adeno-associated virus-mediated knockdown of STING in vivo exhibits protective effects against alcoholic liver injury

Recombinant adeno-associated viral (rAAV) vectors derived from alternative serotypes are a powerful tool to deliver genes globally to a target tissue(s) (McCarty et al., 2003; Nakai et al., 2005). To identify the function of STING knockdown in mice, an adeno-associated virus-8 (AAV8) vector was administered systemically in the mice to generate the STING knockdown model. The eGFP signal in the liver transfected with STING knockdown plasmid. First, the effective delivery of rAAV8-STING to mice livers was confirmed using fluorescent microscopy and western blot analysis, which showed efficient transduction in the liver 14 days after rAAV administration (Figure 3a,b). Histological analyses of the liver using H&E and oil red O staining revealed reduced steatosis and necrosis in the liver following rAAV8-STING administration. Knockdown of STING in the liver tissue inhibited apoptosis, steatosis and ballooning to a greater extent in the rAAV8-STING-treated mice compared to the rAAV8-empty-treated mice in the EtOH-fed group (Figure 3c,d). Moreover, the serum AST, ALT and TG levels were downregulated in the rAAV8-STING-treated EtOH-fed mice (Figure 3e–g).

To explore the functional effects of STING knockdown in Gao binge ethanol model, we evaluated the circulation levels of inflammatory cytokines in the serum and primary KCs of rAAV8-STING-treated and rAAV8-empty-treated mice. Our data show that deficiency of STING greatly decreases the levels of proinflammatory cytokines, including TNF-α , IL-6, and IL-1β in the EtOH-fed group (Figure 3h,i). Figure 3j shows that hepatocyte apoptosis was attenuated in the STING-knockdown mice in the EtOH-fed group as indicated by a reduced Bax/Bcl2 ratio and cleaved-caspase3 protein expression. These results confirm that STING knockdown may exert a protective role in Gao binge ethanol model.

3.4 | Treatment with STING agonist worsens alcoholic liver injury in the Gao binge ethanol model

CD-fed and EtOH-fed mice were treated with DMXAA (25 mg/kg/2 days, ip) for 16 days. At the end of the experiment, DMXAA treatment did not have a significant effect on the body weight of the mice (Figure 4a). H&E, oil red O, and TUNEL staining revealed DMXAA induced steatosis, infiltration of inflammatory cells and hepatocyte apoptosis (Figure 4b,c). DMXAA exposure led to significantly increase in the serum levels of AST, ALT and TG (Figure 4d–f) as well as expression of IL-1β, TNF-α, and IL-6 in primary KCs and serum (Figure 4g,h). Activation of STING in the liver promotes hepatocyte apoptosis, indicated by an increased Bax/Bcl2 ratio and cleaved-caspase3 protein levels (Figure 4i). Taken together, these results indicate that STING activation induces hepatocyte apoptosis and inflammation in the livers of mice.

3.5 | STING promotes the pro-inflammatory responses of RAW264.7 cells

Inflammatory responses greatly affect the initiation of macrophage activation in the Gao binge ethanol model. Therefore, we assessed the potential role of STING in inflammatory responses in macrophages. Incubation with DMXAA enhanced the levels of IL-6, IL-1β, and TNF-α in the RAW264.7 cells (Figure 5a,b). Furthermore, we used STING-siRNA transfection to confirm the ability of STING to inhibit liver injury in the mouse livers, and Figure S2A shows the successful transfection efficiency of STING-siRNA in RAW264.7 cells. Our results show that the knockdown of STING markedly inhibits the upregulation of IL-6, IL-1β, and TNF-α (Figure 5c,d). Next, we used the pEGFP-STING plasmid to overexpress STING in the RAW264.7 cells (Figure S2C). Forced ectopic expression of STING led to elevated levels of inflammatory cytokines IL-6, IL-1β, and TNF-α (Figure 5e,f). These data suggest that excessive activation of STING signng may induce systemic inflammation.

3.6 | STING-driven macrophage factors enhance hepatocyte apoptosis

Our study revealed that mtDNA activates KCs via the binding of STING, further aggravating liver injury. It has been reported that acetaminophen overdose causes neutrophils to accelerate inflammatory response, proinflammatory cytokines, and in turn, speed up the death of hepatocyte (He et al., 2017). To validate whether STING-driven macrophage factors influence hepatocyte apoptosis, we treated the RAW264.7 cells with and without mtDNA and incubated AML12 cells with the RAW264.7 cells-CM (culture medium). The AML12 cells incubated with the CM of mtDNA-treated RAW264.7 cells showed a greater increase in the Bax/Bcl2 ratio and cleaved-caspase3 protein levels compared to that in the AML12 cells incubated with control-treated RAW264.7 cells-CM (Figure 6a). Furthermore, flow cytometry and TUNEL staining also showed that the number of apoptotic cells was increased (Figure 6b,c). Together, these results suggest that STING activation enables macrophages to secrete factors that may enhance hepatocyte apoptosis.

3.7 | mtDNA-mediated regulation of macrophage activation by STING-TBK1-IRF3/NF-κB pathway in the Gao binge ethanol administration in mice

It has been demonstrated that STING and its downstream NF-κB and IRF3 trigger inflammatory reaction in response to the presence of cytosolic DNA (Liu et al., 2021). We assessed the protein expression levels of phosphorylation of TBK1, P-65 NF-κB, and IRF3 in mouse

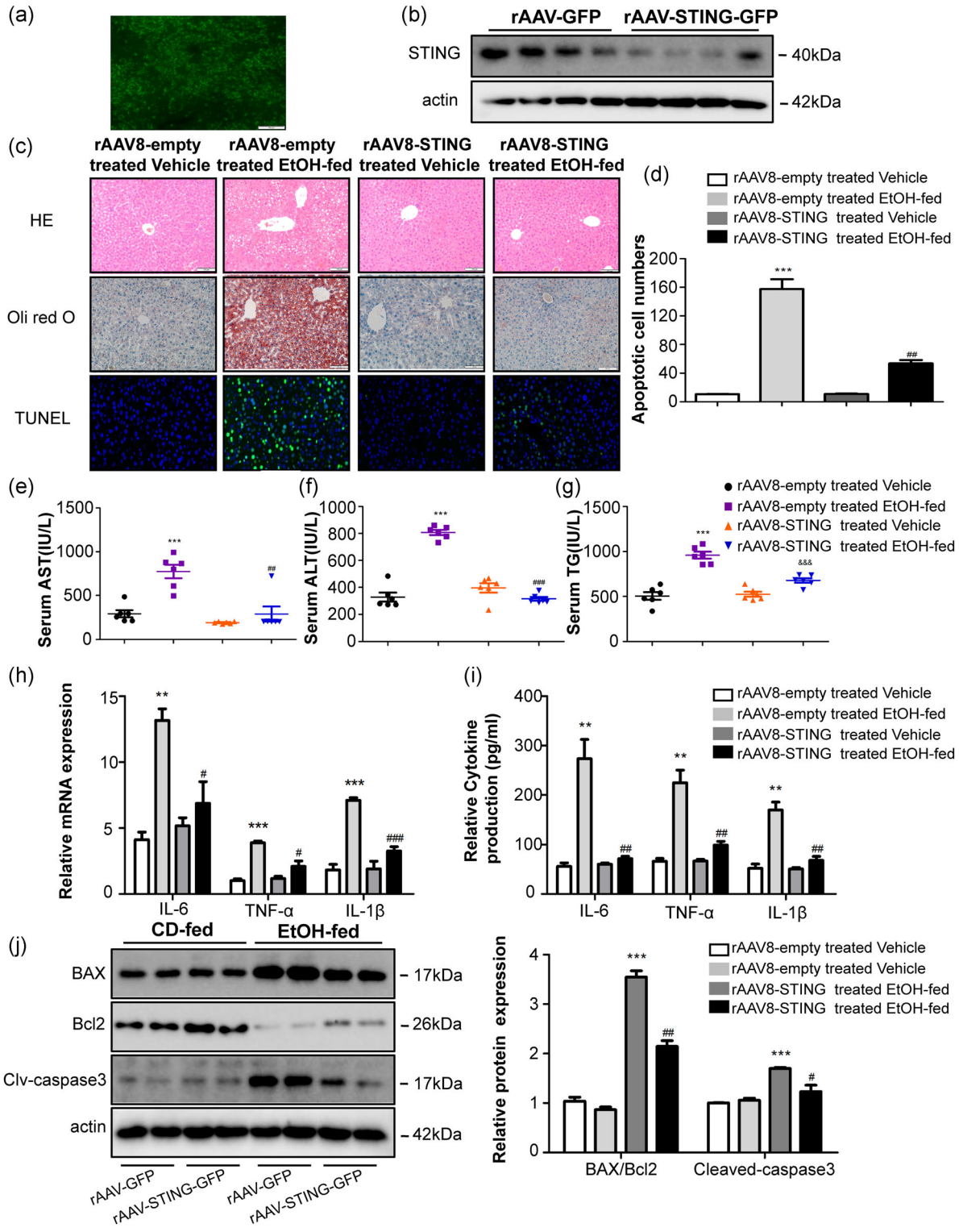

FIGURE 3 Deficiency of STING attenuated inflammation and liver damage in Gao binge ethanol model. Fluorescence microscopy (a) and western blot analysis (b) revealed efficient transduction of rAAV-STING-GFP in mice livers and primary KCs. Pathological observation using H&E, Oil Red, and TUNEL staining. Scale bars: 100, 100, 50 μm (c, d). Graphs show the levels of AST (e), ALT (f), and TG (g) in serum. Graphs show the expression of TNF-α, IL-6, and IL-1β at mRNA in primary KCs (h) and the circulation levels of TNF-α, IL-6, and IL-1β in serum (i). Protein levels of Bax, Bcl2, caspase3, and cleaved-caspase3 (j). $n = 6$ in each group. Values are shown as mean ± SD. $^{**}p < 0.01$, $^{***}p < 0.001$ compared to rAAV8-empty treated vehicle group, $^{\#}p < 0.05$, $^{\#\#}p < 0.01$, $^{\#\#\#}p < 0.001$ compared to rAAV8-empty treated EtOH-fed group. For all panels, data represent the mean ± SEM for three independent experiments. ALT, alanine aminotransferase; AST, aspartate aminotransferase; H&E, hematoxylin and eosin; KC, Kupffer cell; mRNA, messenger RNA

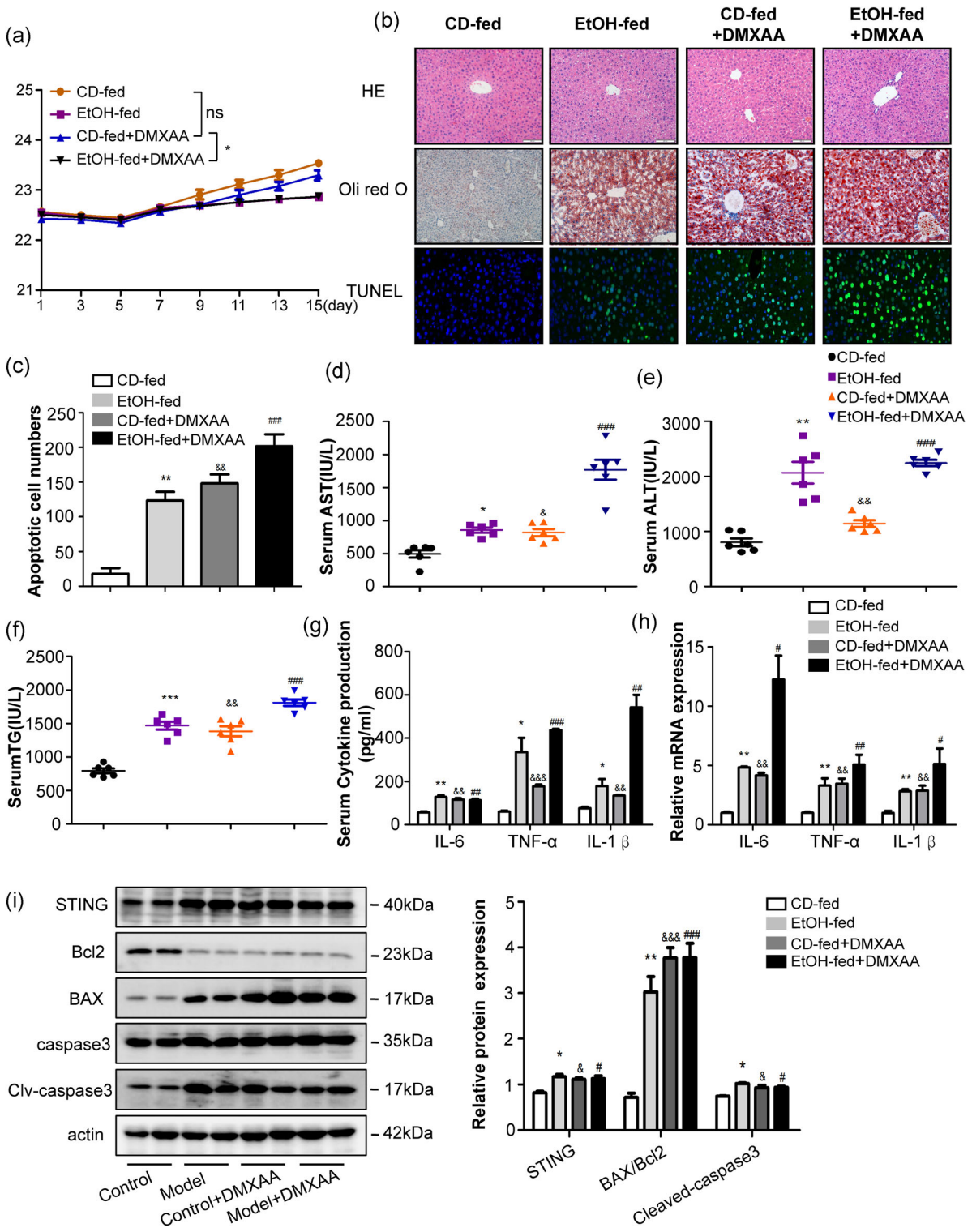

FIGURE 4 DMXAA induced apoptosis and inflammation in the livers of mice. WT mice were treated with DMXAA for 16 days. Graphs show the body weight (a). Representative H&E, Oil Red staining and Tunel staining of liver tissue sections (b, c). Scale bars: 100, 100, and 50 μm. Serum AST, ALT and TG levels (d–f). The circulation levels of proinflammatory cytokines, including TNF-α, IL-1β, and IL-6 were determined by ELISA in serum (g). The mRNA levels of TNF-α, IL-1β, and IL-6 were detected by RT-qPCR in primary KCs (h). Protein levels of Bax, Bcl2, caspase3, and cleaved-caspase3 (i). $n = 6$ in each group. Values are shown as mean ± SEM. $^{*}p < 0.05$, $^{**}p < 0.01$, $^{***}p < 0.001$ compared to CD-fed group, $^{\&}p < 0.05$, $^{\&\&}p < 0.01$, $^{\&\&\&}p < 0.001$ compared to CD-fed group. $^{\#}p < 0.05$, $^{\#\#}p < 0.01$, $^{\#\#\#}p < 0.001$ compared to CD-fed group. For all panels, data represent the mean ± SEM for three independent experiments. ALT, alanine aminotransferase; AST, aspartate aminotransferase; DMXAA,; ELISA, enzyme-linked immunosorbent assay; H&E, hematoxylin and eosin; KC, Kupffer cell; mRNA, messenger RNA

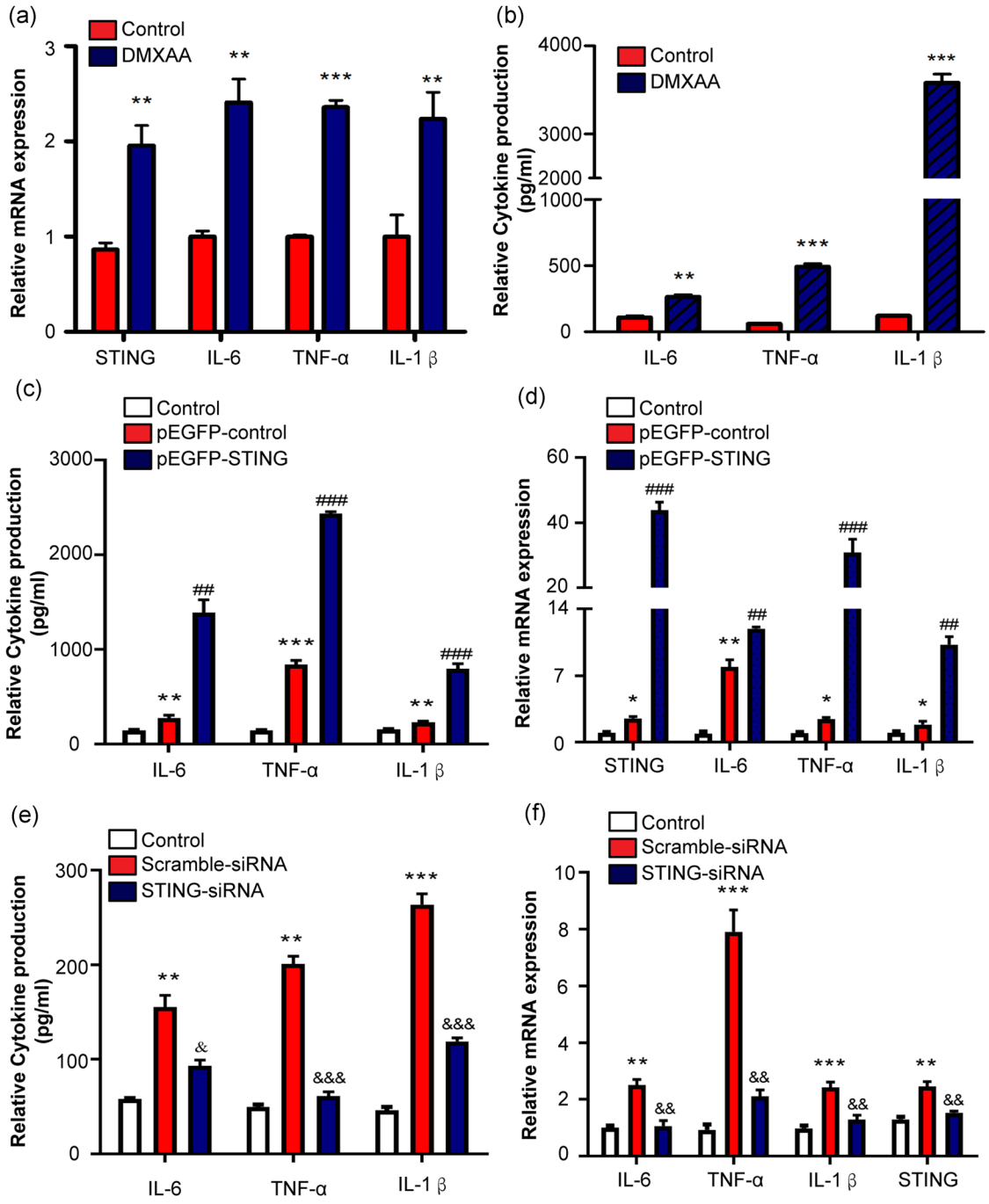

FIGURE 5 Effect of STING overexpression and knockdown on inflammatory responses of RAW264.7 cells. RAW264.7 cells were stimulated with or without DMXAA (100 μg/ml) for 24 h. The cell lysates and culture supernatant were collected 24 h after DMXAA treatment to evaluate the levels of proinflammatory cytokines (IL-1β, IL-6, and TNF-α). The mRNA levels of proinflammatory cytokines were detected by RT-qPCR in RAW264.7 cells (a) and the secretion of proinflammatory cytokines was determined by ELISA in culture supernatant (b). RAW264.7 cells were transfected with pEGFP-STING and treated with mtDNA (100 ng/ml). The levels of IL-1β, IL-6, and TNF-α were detected by ELISA (c) and real time-PCR (d). RAW264.7 cells were transfected with STING-siRNA and treated with mtDNA. Protein and mRNA levels were determined by ELISA (e) and real-time PCR (f). $^{*}p < 0.05$, $^{**}p < 0.01$, $^{***}p < 0.001$ compare to Control group, $^{\#\#}p < 0.01$, $^{\#\#\#}p < 0.001$ compare to pEGFP-control group, $^{\&}p < 0.05$, $^{\&\&}p < 0.01$, $^{\&\&\&}p < 0.001$ compare to compare to Scramble-siRNA group. For all panels, data represent the mean ± SEM for three independent experiments in vitro

livers. Western blot analysis revealed that STING, the phosphorylation of TBK1, P-65 NF-κB, and IRF3 increased in the EtOH-fed group (Figure 7a), indicating the activation of the STING signng pathway in the Gao binge ethanol model. Moreover, treatment of RAW264.7 cells with mtDNA induced TBK1, P-65 NF-κB, and IRF3 phosphorylation in vitro (Figure 7b). To assess the effects of STING on IRF3 and NF-κB pathway activation, we analyzed the STING signng pathway in RAW264.7 cells treated with the pEGFP-STING plasmid,

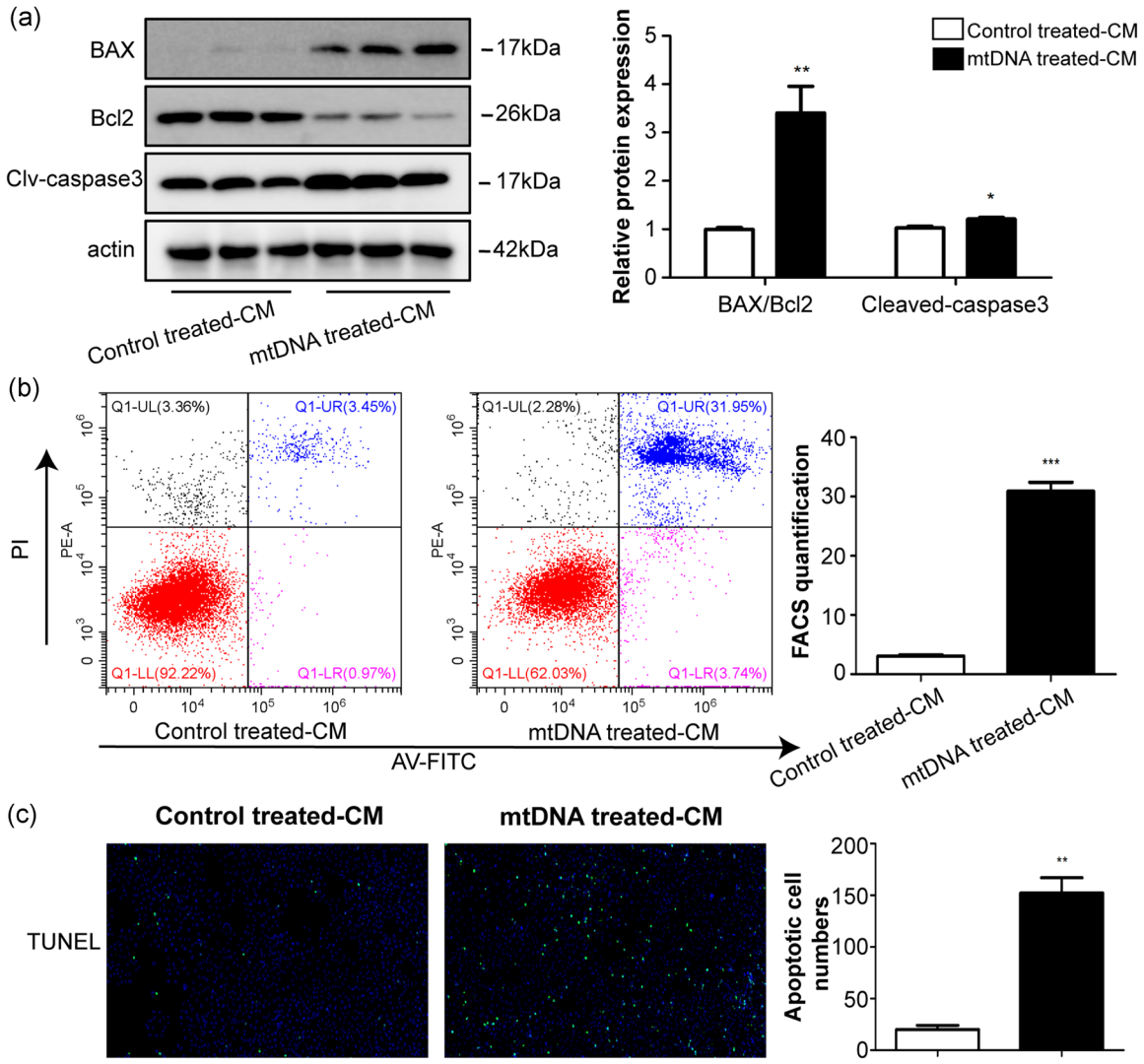

FIGURE 6 Macrophage factors regulate hepatocyte apoptotic responses. CM were collected from mtDNA-treated RAW264.7 cells and control-treated RAW264.7 cells. CM were mixed with fresh media in a 1:1 ratio and supplemented with AML12 cells for 48 h. The apoptosis-associated protein levels were examined using western blot analysis (a). Apoptosis was determined by flow cytometry (b) and TUNEL staining (c). $^{*}p < 0.05$, $^{**}p < 0.01$, $^{***}p < 0.001$ compare to control treated-CM group. For all panels, data represent the mean ± SEM for three independent experiments in vitro

which promoted STING overexpression, as well as, TBK1 phosphorylation, IRF3 phosphorylation, and p65 NF-κB phosphorylation (Figure 7c). STING-siRNA were transiently transfected into RAW264.7 cells for 24 h. Figure 7d shows that STING-targeted therapy in vivo significantly inhibited the STING signng pathway. These results indicate that STING-TBK1-IRF3/NF-κB pathway activation in macrophages contributes to inflammation.

4 | DISCUSSION

Alcoholic liver injury is a liver disease caused by long-term heavy drinking (Fuster & Samet, 2018). KCs are the resident macrophages of the liver involved in the process of alcoholic liver injury by activating pathways that lead to the production of chemokines and cytokines (L. Dou et al., 2019; Slevin et al., 2020). KCs account for approximately 80% of the total macrophages in the body (P. Li et al., 2017). Our study shows that STING is significantly upregulated in KCs isolated from the livers of EtOH-fed mice.

Recent studies on sterile inflammation have suggested various potential therapeutic targets for alcoholic liver injury. Changes in the intestinal microbiome composition lead to an increase in the levels of pathogen-associated molecular patterns and alcohol metabolites further generating DAMPs, which activate inflammatory pathways that trigger ALD (Mihm, 2018; Shim et al., 2020). Previous studies have shown that the mtDNA is recognized as foreign particle in the body, and thus leads to the activation of the innate immune system (Lood et al., 2016). We observed that mtDNA released by the apoptotic hepatocytes which promote KCs inflammation via the activation of STING, also induces a feedback pathway to aggravate liver

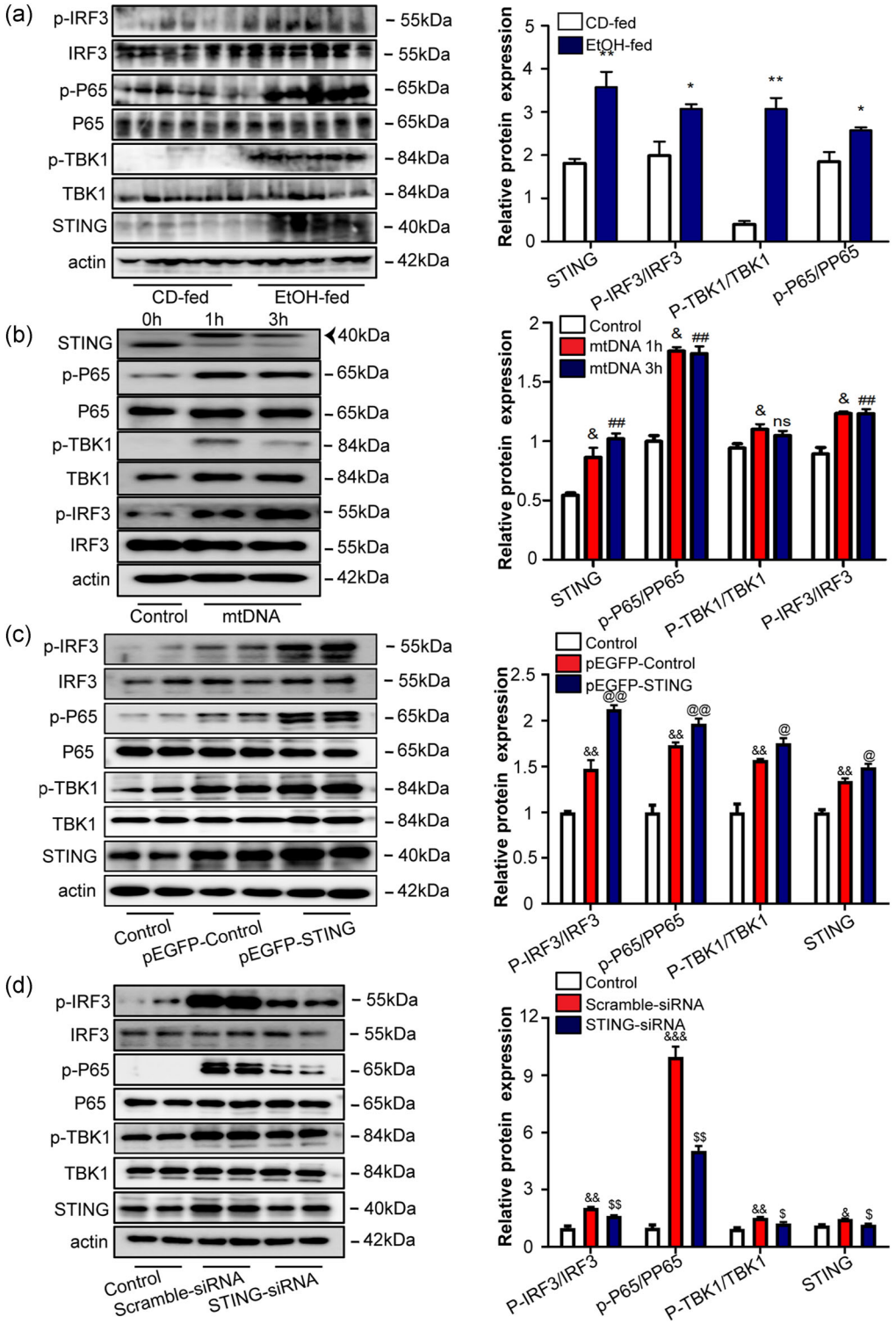

FIGURE 7 mtDNA-mediated STING-TBK1-IRF3/NF-κB signal activation in Gao binge ethanol model and RAW264.7 cells. The expression of STING, TBK1, phosphorylated TBK1 (p-TBK1), phosphorylated IRF3(p-IRF3), NF-κBp65 phosphorylated (p-NF-κBp65), NF-κBp65, and β-actin in the CD-fed and EtOH-fed mice was determined by western blot analysis (a). RAW264.7 cells were stimulated with 100 ng/ml of mtDNA for 1 or 3 h, and the signng response was determined by immunoblotting for STING, IRF3, p-IRF3, TBK1, p-TBK1, NF-κBp65, and p- NF-κBp65 with β-actin serving as a loading control (b). The proteins were extracted 24 h after transfection of activated RAW264.7 cells with pEGFP-STING plasmid or STING-RNAi. Protein level of STING, TBK1, phosphorylated TBK1 (p-TBK1), phosphorylated IRF3 (p-IRF3), phosphorylated NF-κBp65 (p-NF-κBp65), NF-κBp65, and β-actin were measured by western blot analysis (c, d). $^{*}p < 0.05$, $^{**}p < 0.01$ compared to CD-fed group, $^{\&}p < 0.05$, $^{\&\&}p < 0.01$ compared to control group, $^{\#\#}p < 0.01$ compared to control group, $^{@}p < 0.05$, $^{@@}p < 0.01$ compared to pEGFP-Control group, $^{\$}p < 0.05$, $^{\$\$}p < 0.01$ compared to Scramble-siRNA group. For all panels, data represent the mean ± SEM for three independent experiments

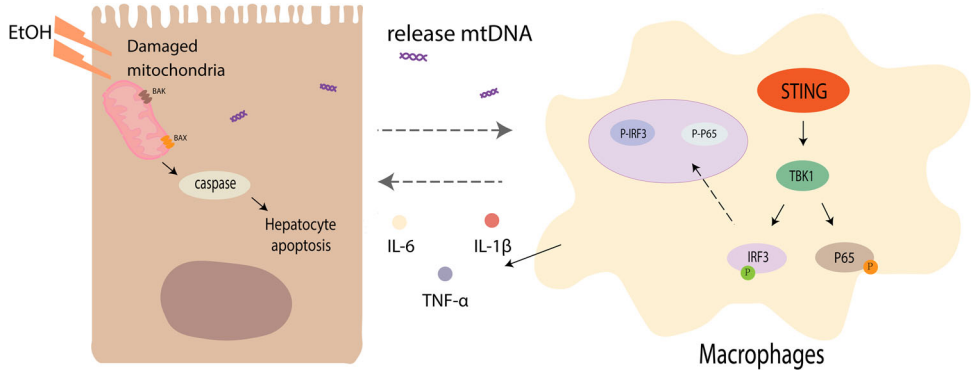

FIGURE 8 Hepatic mtDNA-STING promotes inflammation and hepatocyte apoptosis in Gao binge ethanol model. mtDNA released by hepatocytes undergoing apoptosis activates macrophages which induces IL-1β, TNF-α, and IL-6 expression by regulating the STING-TBK1-IRF3/NF-κB pathway, thereby further aggravating liver injury. mtDNA, mitochondrial DNA

injury. STING activation markedly upregulates the expression of proinflammatory factors IL-1β, IL-6, and TNF-α which in turn aggravate hepatocyte apoptosis. To further understand the function of STING in Gao binge ethanol model, we used liver-specific STING knockdown mice. Our data revealed that STING deficiency alleviated inflammatory infiltration and liver injury to a greater extent in EtOH-fed mice compared to that in the control mice. Furthermore, DMXAA injection in WT mice led to hepatocyte apoptosis and inflammatory infiltration in the liver.

Zhao et al. (2018) showed that the DNA released from apoptotic acinar cells is sensed by STING in leukocytes and leads to the activation of downstream proinflammatory cytokines in experimental acute pancreatitis. Activation of STING has been shown to induce T cell apoptosis in sepsis and trauma (Long et al., 2020). STING upregulates the proinflammatory cytokines, and STING knockout alleviates the inflammatory response and facilitates recovery in spinal cord injury. In summary, STING gene does play an important role in immune response and apoptosis. We provide a new perspective for alcoholic liver injury from the perspective of aseptic inflammation.

Recently, a role for STING-TBK1-IRF3/NF-κB signng in cancer progression has been identified (Kwon & Bakhoum, 2020). STING recruit and activate TBK1. In turn, TBK1 transphosphorylates IRF3 and NFκB, at which point IRF3 and NFκB translocate to the nucleus and driven inflammatory genes (Bai & Liu, 2019). Our data shows that activated STING induces the production of proinflammatory cytokines through the STING-TBK1-IRF3/NF-κB pathway in Gao binge ethanol model. Forced STING expression could utilize IRF3 and NF-κB pathways to promote its effects on proinflammatory genes.

Although the pathogenesis of alcoholic liver injury has been extensively studied, very few limited effective preventive and curative treatments have been developed so far. Thus, the findings of our study provide new insights into the prevention and treatment of alcoholic liver injury. However, STING-mediated inflammation in the Gao binge ethanol model dependent on IRF3 or NF-κB needs to be further investigated.

5 | CONCLUSION

In summary, we have shown that macrophage STING signaling plays an important role in Gao binge ethanol model. Alcohol metabolism cause hepatocyte apoptosis and release of mtDNA which can activate STING signaling in macrophages and promote inflammatory cytokines. Moreover, our data indicate that STING signaling-activated macrophages cause further liver injury as evidenced by increased apoptotic protein activation in liver tissue (Figure 8).

ACKNOWLEDGMENTS

All authors thank PhD. Dandan Zang and PhD. Li Liu of the Center for Scientific Research of Anhui Medical University for valuable help in our work. This study was supported by the National Science Foundation of China (U19A2001) and the University Synergy Innovation Program of Anhui Province (GXXT-2020-063).

CONFLICT OF INTERESTS

The authors declare that there are no conflict of interests.

AUTHOR CONTRIBUTIONS

Ling Wang, Hong-Mei You, and Hong-Wu Meng conceived and carried out experiments, analyzed data, and wrote the manuscript. Xue-Yin Pan, Xin Chen, and Yi-Hui Bi provided technical assistance during the experiment. Juan-Juan Li, Ya-Fei Zhang, Zheng-Wei Zhang, and Na-Na Yin isolated Kupffer cells and primary hepatocytes. Cheng Huang and Jun Li participated in the design of this study and revised the manuscript. All authors contributed to the writing of the manuscript.

DATA AVAILABILITY STATEMENT

Data are available on request to the authors.

ORCID

Jun Li http://orcid.org/0000-0001-7541-752X

REFERENCES

Abe, T., & Barber, G. J. J. ov (2014). Cytosolic-DNA-mediated, STING-dependent proinflammatory gene induction necessitates canonical NF-κB activation through TBK1. *Journal of Virology*, *88*(10), 5328–5341. https://doi.org/10.1128/jvi.00037-14

Bai, J., Cervantes, C., Liu, J., He, S., Zhou, H., Zhang, B., Cai, H., Yin, D., Hu, D., Li, Z., Chen, H., Gao, X., Wang, F., O'Connor, J. C., Xu, Y., Liu, M., Dong, L. Q., & Liu, F. (2017). DsbA-L prevents obesity-induced inflammation and insulin resistance by suppressing the mtDNA release-activated cGAS-cGAMP-STING pathway. *Proceedings of the National Academy of Sciences of the United States of America*, *114*(46), 12196–12201. https://doi.org/10.1073/pnas.1708744114

Bai, J., & Liu, F. J. D. (2019). The cGAS-cGAMP-STING pathway: A molecular link between immunity and metabolism. *Diabetes*, *68*(6), 1099–1108. https://doi.org/10.2337/dbi18-0052

Barber, G. J. T. ii (2014). STING-dependent cytosolic DNA sensing pathways. *Trends in Immunology*, *35*(2), 88–93. https://doi.org/10.1016/j.it.2013.10.010

Bennett, K., Enki, D., Thursz, M., Cramp, M., & Dhanda, A. D. (2019). Systematic review with meta-analysis: high mortality in patients with non-severe alcoholic hepatitis. *Alimentary pharmacology & therapeutics*, *50*(3), 249–257. https://doi.org/10.1111/apt.15376

Bertola, A., Mathews, S., Ki, S., Wang, H., & Gao, B. J. N. p (2013). Mouse model of chronic and binge ethanol feeding (the NIAAA model). *Nature Protocols*, *8*(3), 627–637. https://doi.org/10.1038/nprot.2013.032

Cai, Y., Xu, M. J., Koritzinsky, E. H., Zhou, Z., Wang, W., Cao, H., Yuen, P. S., Ross, R. A., Star, R. A., Liangpunsakul, S., & Gao, B. (2017). Mitochondrial DNA-enriched microparticles promote acute-on-chronic alcoholic neutrophilia and hepatotoxicity. *JCI Insight*, *2*(14):e92634. https://doi.org/10.1172/jci.insight.92634

Chen, Q., Sun, L., & Chen, Z. J. N. i (2016). Regulation and function of the cGAS-STING pathway of cytosolic DNA sensing. *Nature Immunology*, *17*(10), 1142–1149. https://doi.org/10.1038/ni.3558

Cheng, A. N., Cheng, L. C., Kuo, C. L., Lo, Y. K., Chou, H. Y., Chen, C. H., Wang, Y. H., Chuang, T. H., Cheng, S. J., & Lee, A. Y. (2020). Mitochondrial Lon-induced mtDNA leakage contributes to PD-L1-mediated immunoescape via STING-IFN signaling and extracellular vesicles. *Journal for Immunotherapy of Cancer*, *8*(2):e001372. https://doi.org/10.1136/jitc-2020-001372

Dou, L., Shi, X., He, X., & Gao, Y. J. F. ii (2019). Macrophage phenotype and function in liver disorder. *Frontiers in Immunology*, *10*, 3112. https://doi.org/10.3389/fimmu.2019.03112

Dou, Z., Ghosh, K., Vizioli, M. G., Zhu, J., Sen, P., Wangensteen, K. J., Simithy, J., Lan, Y., Lin, Y., Zhou, Z., Capell, B. C., Xu, C., Xu, M., Kieckhaefer, J. E., Jiang, T., Shoshkes-Carmel, M., Tanim, K., Barber, G. N., Seykora, J. T.,, … Berger, S. L. (2017). Cytoplasmic chromatin triggers inflammation in senescence and cancer. *Nature*, *550*(7676), 402–406. https://doi.org/10.1038/nature24050

Fang, C., Mo, F., Liu, L., Du, J., Luo, M., Men, K., Na, F., Wang, W., Yang, H., & Wei, X. (2020). Oxidized mitochondrial DNA sensing by STING signaling promotes the antitumor effect of an irradiated immunogenic cancer cell vaccine. *Cellular & Molecular Immunology*, *18*, 2211–2223. https://doi.org/10.1038/s41423-020-0456-1

Fuster, D., & Samet, J. H. (2018). Alcohol use in patients with chronic liver disease. *The New England Journal of Medicine*, *379*(13), 1251–1261. https://doi.org/10.1056/NEJMra1715733

Grabherr, F., Grander, C., Adolph, T. E., Wieser, V., Mayr, L., Enrich, B., Macheiner, S., Sangineto, M., Reiter, A., Viveiros, A., Zoller, H., Bufler, P., Moschen, A. R., Dinarello, C. A., & Tilg, H. (2018). Ethanol-mediated suppression of IL-37 licenses alcoholic liver disease. *Liver International*, *38*(6), 1095–1101. https://doi.org/10.1111/liv.13642

He, Y., Feng, D., Li, M., Gao, Y., Ramirez, T., Cao, H., Kim, S. J., Yang, Y., Cai, Y., Ju, C., Wang, H., Li, J., & Gao, B. (2017). Hepatic mitochondrial DNA/Toll-like receptor 9/MicroRNA-223 forms a negative feedback loop to limit neutrophil overactivation and acetaminophen hepatotoxicity in mice. *Hepatology*, *66*(1), 220–234. https://doi.org/10.1002/hep.29153

Holt, M., Cheng, L., & Ju, C. J. J. olb (2008). Identification and characterization of infiltrating macrophages in acetaminophen-induced liver injury. *Journal of Leukocyte Biology*, *84*(6), 1410–1421. https://doi.org/10.1189/jlb.0308173

Kwon, J., & Bakhoum, S. J. C. d (2020). The cytosolic DNA-sensing cGAS-STING pathway in cancer. *Cancer Discovery*, *10*(1), 26–39. https://doi.org/10.1158/2159-8290.Cd-19-0761

Li, H. D., Chen, X., Xu, J. J., Du, X. S., Yang, Y., Li, J. J., Yang, X. J., Huang, H. M., Li, X. F., Wu, M. F., Zhang, C., Zhang, C., Li, Z., Wang, H., Meng, X. M., Huang, C., & Li, J. (2020). DNMT3b-mediated methylation of ZSWIM3 enhances inflammation in alcohol-induced liver injury via regulating TRAF2-mediated NF-κB pathway. *Clinical Science*, *134*(14), 1935–1956. https://doi.org/10.1042/cs20200031

Li, P., He, K., Li, J., Liu, Z., & Gong, J. J. M. i (2017). The role of Kupffer cells in hepatic diseases. *Molecular Immunology*, *85*, 222–229. https://doi.org/10.1016/j.molimm.2017.02.018

Liu, Y., Lu, X., Qin, N., Qiao, Y., Xing, S., Liu, W., Feng, F., Liu, Z., & Sun, H. (2021). STING, a promising target for small molecular immune modulator: A review. *European Journal of Medicinal Chemistry*, *211*, 113113. https://doi.org/10.1016/j.ejmech.2020.113113

Long, J., Yang, C., Zheng, Y., Loughran, P., Guang, F., Li, Y., Liao, H., Scott, M. J., Tang, D., Billiar, T. R., & Deng, M. (2020). Notch signaling protects CD4 T cells from STING-mediated apoptosis during acute systemic inflammation. *Science Advances*, *6*(39):eabc5447. https://doi.org/10.1126/sciadv.abc5447

Lood, C., Blanco, L. P., Purmalek, M. M., Carmona-Rivera, C., De Ravin, S. S., Smith, C. K., Malech, H. L., Ledbetter, J. A., Elkon, K. B., & Kaplan, M. J. (2016). Neutrophil extracellular traps enriched in oxidized mitochondrial DNA are interferogenic and contribute to lupus-like disease. *Nature Medicine*, *22*(2), 146–153. https://doi.org/10.1038/nm.4027

Ma, J., Cao, H., Rodrigues, R. M., Xu, M., Ren, T., He, Y., Hwang, S., Feng, D., Ren, R., Yang, P., Liangpunsakul, S., Sun, J., & Gao, B. (2020). Chronic-plus-binge alcohol intake induces production of proinflammatory mtDNA-enriched extracellular vesicles and steatohepatitis via ASK1/p38MAPKα-dependent mechanisms. *JCI Insight*, *5*(14):e136496. https://doi.org/10.1172/jci.insight.136496

McCarty, D., Fu, H., Monahan, P., Toulson, C., Naik, P., & Samulski, R. J. G. t (2003). Adeno-associated virus terminal repeat (TR) mutant generates self-complementary vectors to overcome the rate-limiting step to transduction in vivo. *Gene Therapy*, *10*(26), 2112–2118. https://doi.org/10.1038/sj.gt.3302134

Mihm, S. (2018). Danger-associated molecular patterns (DAMPs): molecular triggers for sterile inflammation in the liver. *International Journal of Molecular Sciences*, *19*(10):3104. https://doi.org/10.3390/ijms19103104

Nakai, H., Fuess, S., Storm, T., Muramatsu, S., Nara, Y., & Kay, M. A. (2005). Unrestricted hepatocyte transduction with adeno-associated virus serotype 8 vectors in mice. *Journal of Virology*, *79*(1), 214–224. https://doi.org/10.1128/jvi.79.1.214-224.2005

Nakai, H., Iwaki, Y., Kay, M., & Couto, L. B. (1999). Isolation of recombinant adeno-associated virus vector-cellular DNA junctions from mouse liver. *Journal of Virology*, *73*(7), 5438–5447. https://doi.org/10.1128/jvi.73.7.5438-5447.1999

Pan, X. Y., You, H. M., Wang, L., Bi, Y. H., Yang, Y., Meng, H. W., Meng, X. M., Ma, T. T., Huang, C., & Li, J. (2019). Methylation of RCAN1.4 mediated by DNMT1 and DNMT3b enhances hepatic stellate cell activation and liver fibrogenesis through calcineurin/NFAT3 signaling. *Theranostics*, *9*(15), 4308–4323. https://doi.org/10.7150/thno.32710

Shim, Y., & Jeong, W. I. (2020). Recent advances of sterile inflammation and inter-organ cross-talk in alcoholic liver disease. *Experimental & Molecular Medicine*, *52*(5), 772–780. https://doi.org/10.1038/s12276-020-0438-5

Slevin, E., Baiocchi, L., Wu, N., Ekser, B., Sato, K., Lin, E., Ceci, L., Chen, L., Lorenzo, S. R., Xu, W., Kyritsi, K., Meadows, V., Zhou, T., Kundu, D., Han, Y., Kennedy, L., Glaser, S., Francis, H., Alpini, G., & Meng, F. (2020). Kupffer cells: Inflammation pathways and cell-cell interactions in alcohol-associated liver disease. *The American Journal of Pathology*, *190*(11), 2185–2193. https://doi.org/10.1016/j.ajpath.2020.08.014

Stickel, F., Datz, C., Hampe, J., & Bataller, R. J. G., liver. (2017). Pathophysiology and management of alcoholic liver disease: Update 2016. *Gut and Liver*, *11*(2), 173–188. https://doi.org/10.5009/gnl16477

Sun, Y., Zhao, Y., Li, X., Huang, C., Meng, X., & Li, J. J. F. ip. (2018). β-Arrestin 2 promotes hepatocyte apoptosis by inhibiting Akt pathway in alcoholic liver disease. *Frontiers in Pharmacology*, *9*, 1031. https://doi.org/10.3389/fphar.2018.01031

Tang, C., Zundell, J., Ranatunga, S., Lin, C., Nefedova, Y., Del Valle, J., & Hu, C. J. C. r. (2016). Agonist-mediated activation of STING induces apoptosis in malignant B cells. *Cancer Research*, *76*(8), 2137–2152. https://doi.org/10.1158/0008-5472.Can-15-1885

Woo, S. R., Fuertes, M. B., Corrales, L., Spranger, S., Furdyna, M. J., Leung, M. Y., Duggan, R., Wang, Y., Barber, G. N., Fitzgerald, K. A., Alegre, M. L., & Gajewski, T. F. (2014). STING-dependent cytosolic DNA sensing mediates innate immune recognition of immunogenic tumors. *Immunity*, *41*(5), 830–842. https://doi.org/10.1016/j.immuni.2014.10.017

Yu, Y., Liu, Y., An, W., Song, J., Zhang, Y., & Zhao, X. (2019). STING-mediated inflammation in Kupffer cells contributes to progression of nonalcoholic steatohepatitis. *The Journal of Clinical Investigation*, *129*(2), 546–555. https://doi.org/10.1172/jci121842

Zhao, Q., Wei, Y., Pandol, S., Li, L., & Habtezion, A. J. G. (2018). STING signaling promotes inflammation in experimental acute pancreatitis. *Gastroenterology*, *154*(6), 1822–1835. https://doi.org/10.1053/j.gastro.2018.01.065

SUPPORTING INFORMATION

Additional supporting information may be found in the online version of the article at the publisher's website.

How to cite this article: Wang, L., You, H.-M., Meng, H.-W., Pan, X.-Y., Chen, X., Bi, Y.-H., Zhang, Y.-F., Li, J.-J., Yin, N.-N., Zhang, Z.-W., Huang, C., & Li, J. (2022). STING-mediated inflammation contributes to Gao binge ethanol feeding model. *Journal of Cellular Physiology*, 237, 1471–1485. https://doi.org/10.1002/jcp.30606